

To the 80th Anniversary of B.I. Ionin

# Metal-Polymer Nanobiocomposites with Galactose-Containing Stabilizing Matrices: Dimensional Effect in Changes of Molar Mass Parameters

G. P. Aleksandrova<sup>a</sup>, A. S. Boymirzaev<sup>b</sup>, M. V. Lesnichaya<sup>a</sup>,  
B. G. Sukhov<sup>a</sup>, and B. A. Trofimov<sup>a</sup>

<sup>a</sup> Favorskii Irkutsk Institute of Chemistry, Siberian Branch, Russian Academy of Sciences,  
ul. Favorskogo 1, Irkutsk, 664033 Russia  
e-mail: alexa@irioch.irk.ru

<sup>b</sup> Namangan Institute of Engineering and Technology, Namangan, Uzbekistan

Received December 18, 2014

**Abstract**—Molar mass parameters of galactose-containing polysaccharides constituting composites with noble metal nanoparticles have been determined by means of Size-exclusion chromatography (SEC). The composites are self-assembled via specific interaction of the biopolymers with the surface of the metal nanoparticles. The metal content significantly influences the molar mass parameters of the stabilizing polysaccharides. The change of the polymer of polydispersity is due to their redox interaction with the metal ions as well as due to the alkaline-induced degradation. Increasing the nanoparticles number results in the enhanced macromolecules aggregation.

**Keywords:** nanobiocomposite, polysaccharide, nanoparticle, noble metal, molecular mass parameter

**DOI:** 10.1134/S107036321502022X

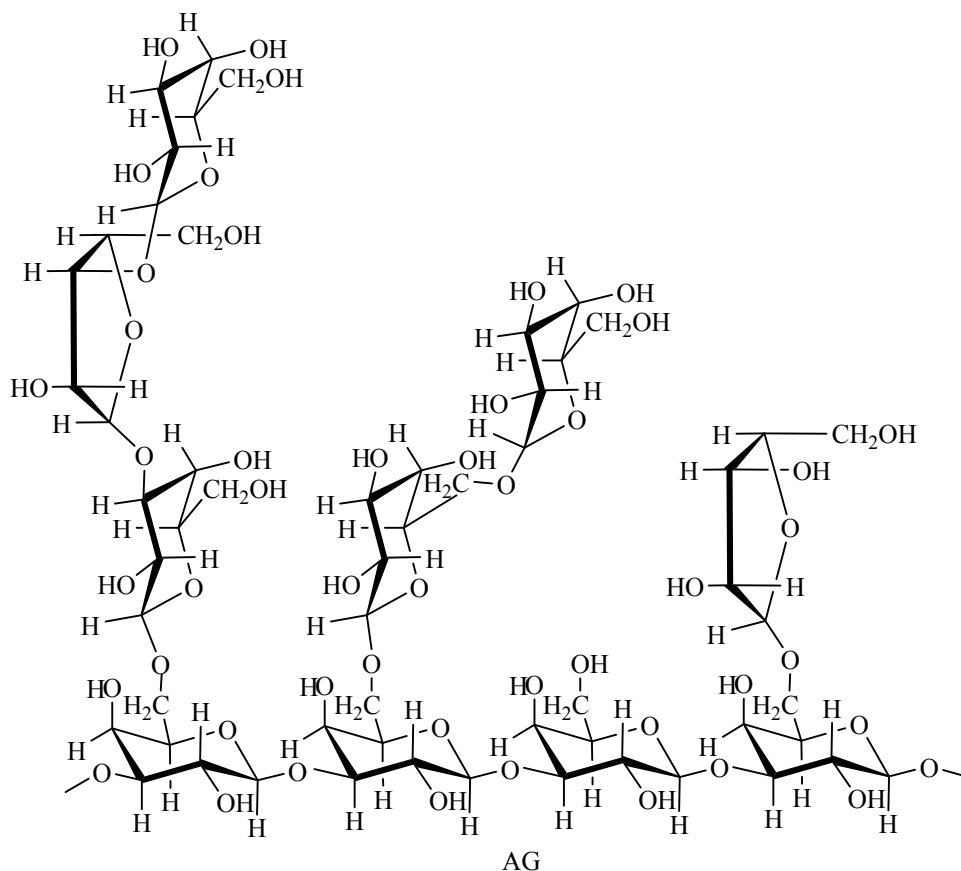
Metal-polymer composites form a class of materials promising for advanced applications, including the biomedical field [1–5]. Natural polymers such as proteins, nucleic acids, and polysaccharides are among widely used matrices to prepare such composites [1–7]. Many polysaccharides including galactose-containing arabinogalactan AG, galactomannan GM, and carrageenan CG can simultaneously act as a stabilizer and a reducing agent [7–10]. Formation of noble metals nanoparticles in the polysaccharide AG, GM, and CG matrices is an efficient approach to prepare biocompatible nanocomposites [9–11]. The dual function of the polysaccharides and possibility to prepare the nanocomposites via the “green” technology makes such biopolymers fairly valuable fine chemistry products [8]. Mechanism of the composites formation as well as the nanoparticles physico-chemical properties have been studied in detail [1–5]; however, another important field is investigation of the polymer matrix change in the course of redox processes

involving the metal precursors [10, 12] and various physical interactions of the macromolecules with the active surface of the formed nanoparticles leading to the nanocomposites self-organization [1, 2]. Study of the mutual influence of the nanoparticles and the polymer stabilizers by means of dynamic and static light scattering has been started in [13].

This work aimed to investigate the influence of the noble metals nanoparticles formed within the polysaccharide matrix on the change of molar mass parameters of the galactose-containing polysaccharides: AG, GM, and CG.

The corresponding composites of zero-valence silver (Ag-AG, Ag-GM, and Ag-CG) and gold (Au-AG, Au-GM, and Au-CG) were prepared under mild conditions elaborated earlier [9]. The metal ions were reduced by hydroxyl and terminal carbonyl groups of the polysaccharides. Identification of silver and gold nanoparticles (their content in the composites being of

Scheme 1.



3.7–11.9%) was performed from X-ray diffraction and electronic absorbance spectroscopy data as described in detail in [9, 10]. Formation of the nanocomposites occurred via specific interactions of the formed metal nanoparticles surface with the polysaccharide macromolecules.

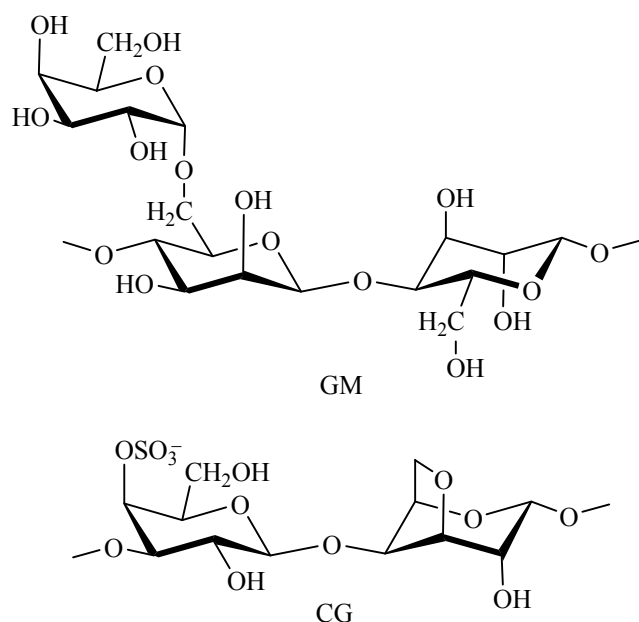
The used galactose-containing polysaccharides differed in the macromolecules structure. Arabino-galactan AG is a natural polysaccharide with the main chain built majorly of the 1→3-linked  $\beta$ -D-galactopyranose units, most of them being branched at the C<sup>6</sup> atoms. The side chains are built from 3,6-di-O-6-substituted fragments of  $\beta$ -D-galactopyranose and 3-O-substituted fragments of  $\beta$ -L-arabinofuranose [14] (Scheme 1).

Galactomannan GM is a comb-like heteropolysaccharide with the main chain consisting of  $\beta$ -D-mannopyranoside units linked via 1→4-glycoside bonds [15]. The side chains were formed by the non-uniformly distributed  $\alpha$ -D-galactopyranose units linked to the mannopyranoside chain via the 1→6-glycoside bonds.

Carrageenan CG is a sulfated polysaccharide with the macromolecule built of the regularly alternating units of 3-O-sulfated  $\beta$ -D-galactopyranose and 4-O-substituted 3,6-anhydro- $\alpha$ -D-galactopyranose [16].

Molar mass parameters of the prepared metal-biopolymer composites were studied by means of size-exclusion chromatography (SEC) taking advantage of three combined detection systems. Formation of the disperse nanoparticles was accompanied by appearance of new links between the in situ formed metal particles and the polysaccharide stabilizers. Moreover, the polysaccharides acted as reducing agents, being oxidized in the course of zero-valence metal formation [12]. The redox processes occurred at pH > 7 upon heating to 90°C; therefore, the macromolecular structure was additionally affected by alkali-induced polymers degradation [17]. A combination of the three simultaneous processes led to changes of the polysaccharides molecular mass parameters. The SEC method gave the information of the molar mass distribution. Using the refractive index (RI) (the signal being related to the polymer concentration in the

Scheme 2.



eluting fractions) allowed determination of the weight-average  $M_w$  and the number-average  $M_n$  molecular mass of the molecules taking into account the universal calibration with the pullulan standards (Fig. 1, curve 1). Details of the universal calibration for SEC analysis of arabinogalactan have been discussed elsewhere [18]. The multi-angle light scattering detector gave the absolute values of  $M_w$  as well as the average gyration radius of the macromolecules; furthermore, it could detect the presence of the macromolecules aggregates (Fig. 1, curve 2). For discussion of the combined use of refractometry and light scattering detectors (MALLS, Mini DAWN TriStar) to determine the absolute values of  $M_w$  and  $M_n$  see [19].

AG revealed the lowest molecular mass of the studied polysaccharides ( $M_p$  42.3 kDa) and was fairly narrow disperse:  $M_w/M_n$  1.06,  $M_w$  45.3 kDa, and  $M_n$  42.6 kDa (see table, Fig. 1a). After the depolymerization under the model conditions (pH 11, 90°C, 15–30 min [12, 17]), it was mostly the number-average molecular mass that decreased ( $M_n$  35.8 kDa), whereas the weight-average molecular mass remained almost constant ( $M_w$  42.8 kDa), and the polydispersity was slightly increased to 1.19 (see data for AG<sub>hydr</sub> in the table).

Polydispersity of GM (see the mass distribution in Fig. 2a) was significantly higher than that of AG ( $M_p$  120.5 kDa,  $t_r$  31.6 мин,  $M_w$  234.4 kDa,  $M_n$  128.8 kDa,

$M_w/M_n$  1.82) (see table). GM macromolecules were highly aggregated, as the peaks observed using the light scattering detector ( $t_r$  26.2 and 29.6 min) had lower retention time than that in the case of RI ( $t_r$  31.6 min). The calculated aggregates radius was of 27 nm.

CG (Fig. 3a) was the most high-molecular polysaccharide of the studied ones ( $M_p$  631.1 kDa,  $t_r$  29.4 min,  $M_w$  1009.0 kDa,  $M_n$  564.7 kDa). Its molecular mass distribution was fairly broad, and the polydispersity index (1.79) was close to that of GM and remarkably exceeded that of AG. The only peak observed using a light scattering detector revealed a somewhat lower retention time ( $t_r$  28.1 min) than that found with a RI. Hence, CG molecules existed majorly in the non-aggregated state.

Analysis of molar mass parameters of silver- and gold-containing composites revealed significant changes in the state of the polysaccharides. The presence of the metal nanoparticles gave rise to the characteristic plasmon absorption at 410 nm (silver) and 530 nm (gold) [1]. The combined use of spectrophotometry detector for SEC analysis allowed observation of the nanoparticles in the nanocomposite fractions. Hence, a hyphenated analysis using refractometry, spectrophotometry, and light scattering detectors could describe the interaction between the metal nanoparticles and polysaccharide macromolecules upon formation of the composite.

In the case of the Ag-AG composites, introduction of a varied amount of silver nanoparticles (3.7–10.7%) resulted in slight (within the method accuracy of 10%) decrease of the molecular mass determined at maximum of the elution peak  $M_p$  (table, samples 3–6). Similar trend was earlier marked in the study of Ag-AG by means of SEC with calibration using dextran standards [12]. Comparison of the  $M_w$  and  $M_n$  values, however, demonstrated steep increase of the polysaccharide polydispersity index from 1.10 (parent AG) to 1.41 (3.7% Ag) and 2.16 (10.7% Ag) (table and Figs. 1a–1d). The enhanced degradation of macromolecules observed during the nanocomposite preparation with increasing silver content was due to acceleration of both the redox reaction and the alkali-induced depolymerization [12, 10]. Noteworthy, the carbonyl and carboxyl groups appearing in the macromolecules due to the redox process were electron acceptors; hence, the glycoside linkage became more reactive towards base hydrolysis, and depolymerization process was further enhanced [10].

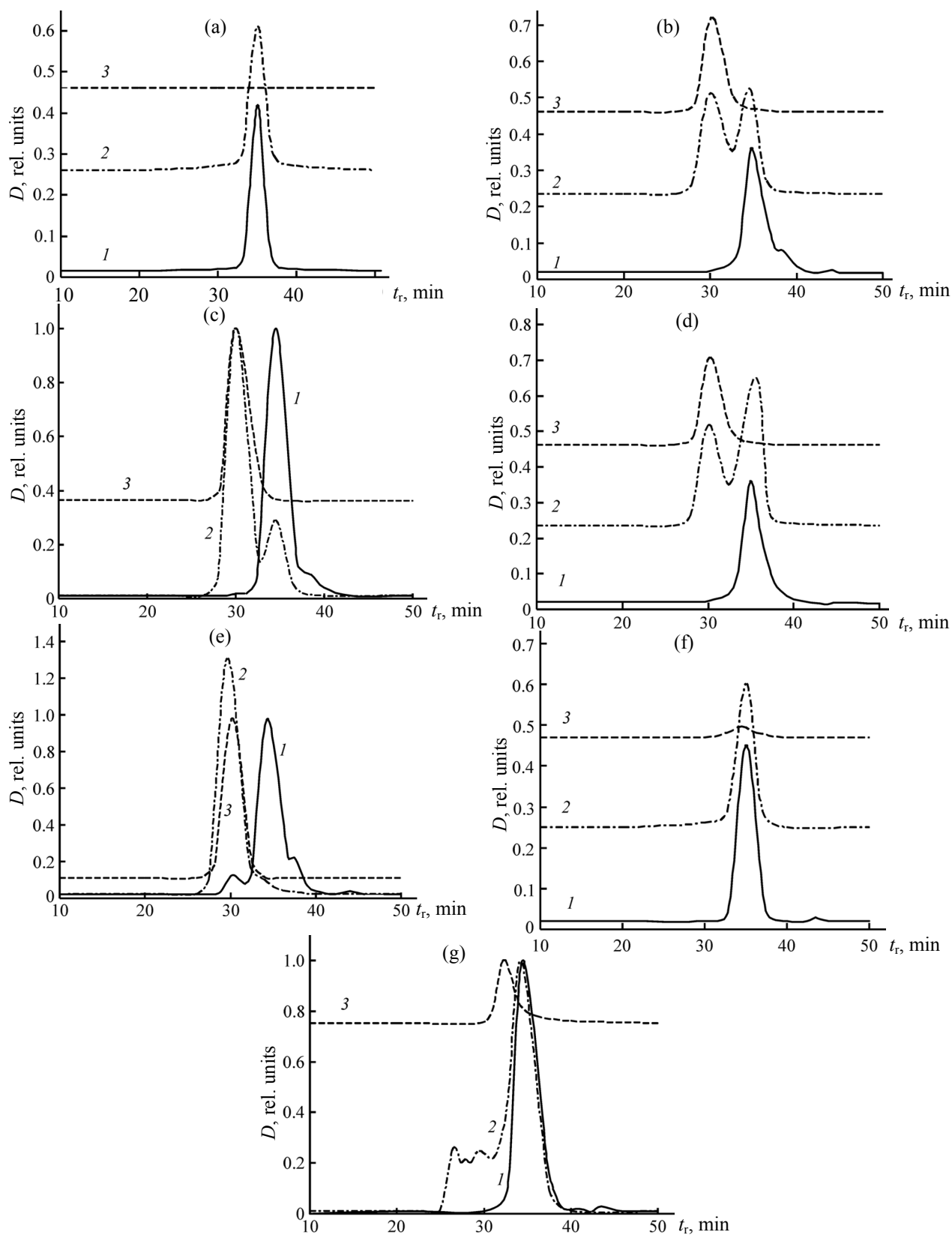


**Fig. 1.** Molecular mass distribution of arabinogalactan (a) and the derived composites with silver Ag-AG (b–e) and gold Au-AG (f, g). Silver content: 3.7 (b), 5.1 (c), 7.0 (d), and 10.7% (e); gold content: 6.7 (f) and 11.9% (g); detector: (1) refractometer, (2) light scattering, and (3) spectrophotometer.

Molar mass parameters of arabinogalactan, galactomannan, carrageenan, and their composites with silver and gold (according to refractometry data)<sup>a</sup>

Run no.	Sample	Me, %	$M_p$	$M_w$	$M_n$	$M_w/M_n$
1	Arabinogalactan AG	—	42.3	45.3	42.6	1.06
2	AG <sub>hydr</sub>	—	41.8	42.8	35.8	1.19
3	Ag-AG	3.7	40.2	40.0	28.4	1.41
4	Ag-AG	5.1	42.2	50.4	37.3	1.35
5	Ag-AG	7.0	44.2	58.3	44.4	1.31
6	Ag-AG	10.7	38.0	39.9	18.5	2.16
7	Au-AG	6.7	42.3	43.8	40.4	1.09
8	Au-AG	11.9	37.5	48.5	35.1	1.38
9	Galactomannan GM	—	120.5	234.4	128.8	1.82
10	Ag-GM	7.0	45.6	89.5	38.0	2.35
11	Au-GM	4.2	62.5	193.7	65.6	2.95
12	Carrageenan CG	—	631.1	1009.0	564.7	1.79
13	Ag-CG	4.0	55.9	71.2	58.4	1.22
14	Au-CG	6.0	102.5	129.6	95.8	1.35

<sup>a</sup>  $M_p$ , molecular mass corresponding to maximum of the chromatographic peak;  $M_w$ , weight-average molecular mass;  $M_n$ , number-average molecular mass;  $M_w/M_n$  polydispersity parameter.

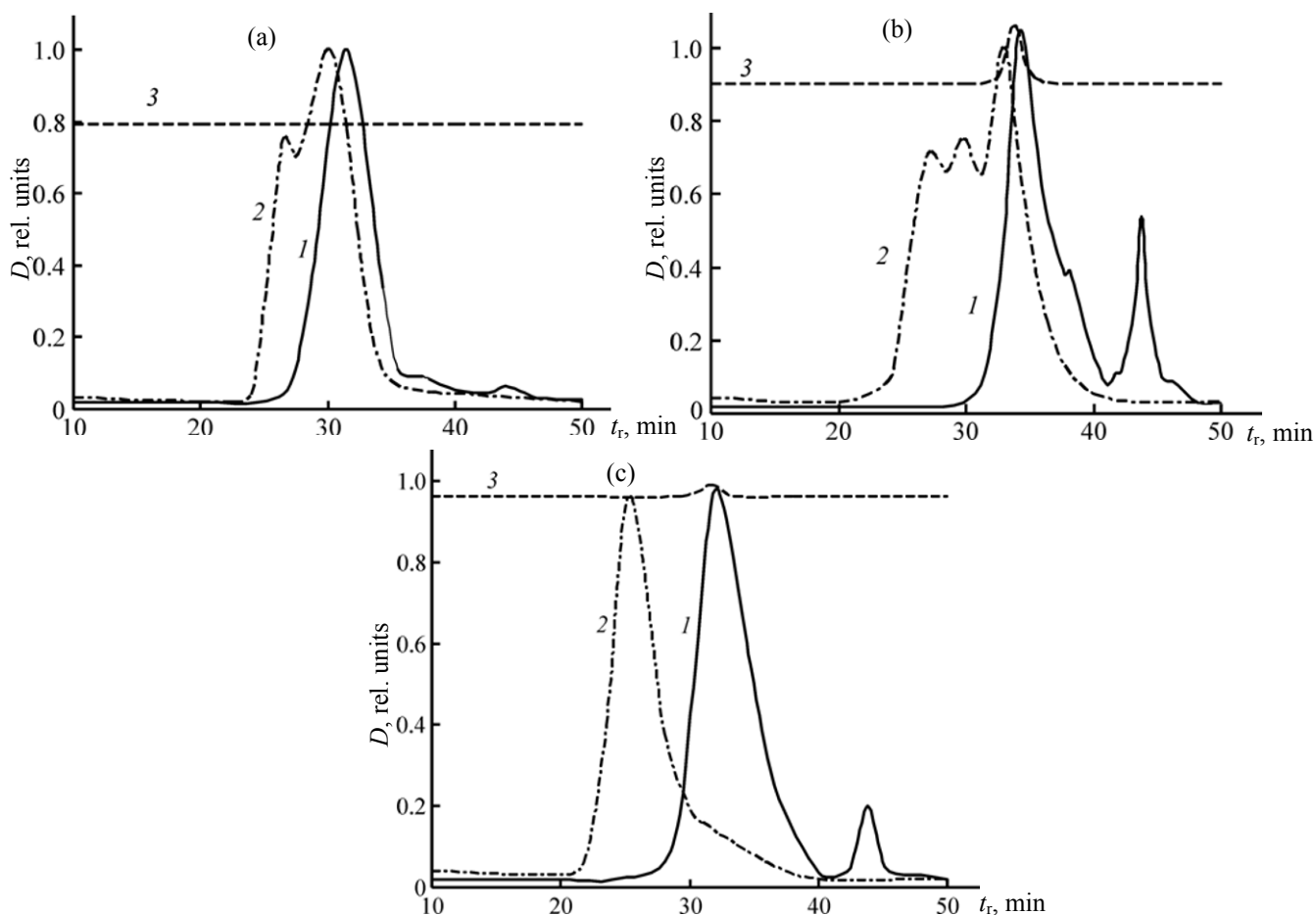


**Fig. 2.** Molecular mass distribution of galactomannan (a) and the derived composites with silver (b) and gold (c). Detector: (1) refractometer, (2) light scattering, and (3) spectrophotometer.

The increase of  $M_w$  values for the samples of Ag-AG containing 5.1 and 7.0% of silver (see table) could be explained by the increased mass of long-chain polysaccharide fractions due to the incorporation of the nanoparticles containing up to several thousand atoms [20]. RI revealed the appearance of the second elution peak in the range of much higher mass during SEC analysis of the Ag-AG sample containing 10.7% of silver (Fig. 1e). The reason for that was evidently the presence of significant fraction of aggregated AG molecules. The fraction of aggregated macromolecules was of 15% as calculated from the ratio of peak areas. The macromolecules aggregation was likely aided by the increased amount of silver nanoparticles being covered with layer of AG. The light scattering detector, the most sensitive to the aggregated macromolecules [13], showed that the retention time of the peak of the parent AG was equal to that of the peak registered with RI. Hence, the pristine polysaccharide did not contain any aggregated macromolecules. In the case of silver-containing composites, the light scattering detector revealed two peaks at  $t_r$  30.3 and 35.0 min. The latter one corresponded to the peak observed with RI, and thus reflected the fraction of free macromolecules not bound to the nanoparticles. The peak at  $t_r$  30.3 min coincided with the peak of silver nanoparticles elution as observed with spectrophotometry detector. With increasing silver content in the composite, that peak grew stronger, as the scattering from the nanoparticles and the aggregated macromolecules was enhanced [13]. At the same time, the peak at  $t_r$  35.0 min became weaker; the free macromolecules fraction was close to zero at silver content of 10.7%.

Using spectrophotometry detector registering a peak at  $t_r$  30.3 min allowed observation of the presence of silver nanoparticles absorbing at 410–430 nm (plasmon resonance), as the polysaccharides were not absorbing at that spectral region. Absorbance intensity at that retention time increased proportionally to the nanoparticles concentration in the composite (Figs. 1b–1d), in accordance with the previously reported data on silver state in the nanocomposites [10]. Hence, combined analysis of SEC data taking advantage of the three-detector system concluded about the interaction (formation of the linkages) between the silver nanoparticles and the stabilizing polysaccharide AG. Increasing number of the nanoparticles in the composite resulted in growing fraction of the aggregated macromolecules. We earlier demonstrated that the nanoparticles size as determined

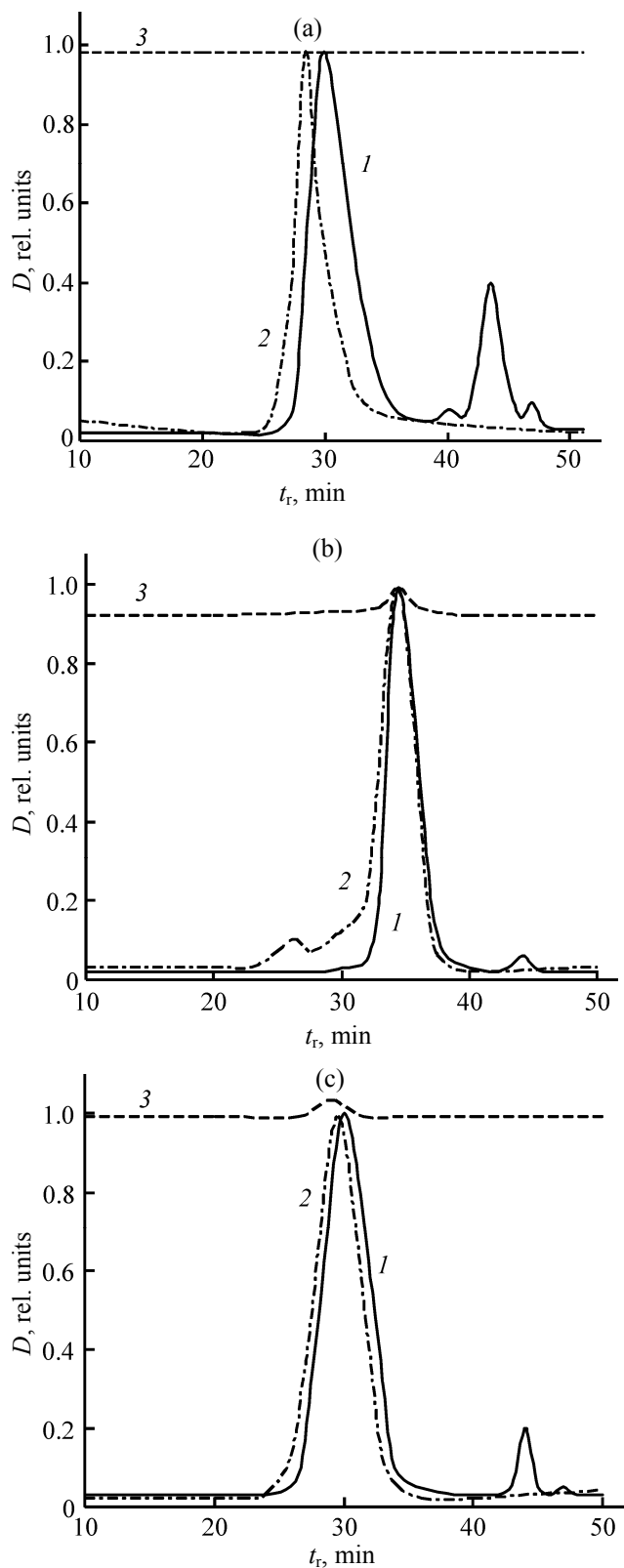


**Fig. 3.** Molecular mass distribution of carrageenan (a) and the derived composites with silver (b) and gold (c). Detector: (1) refractometer, (2) light scattering, and (3) spectrophotometer.

from TEM or X-ray diffraction data increased with their content in the composite [20]. Correspondingly, their surface area increased, and it required more of the polysaccharide to prevent aggregation. As a result, the aggregation was enhanced, and that was reflected in SEC data.

In the case of the Au-AG composite containing 6.7% of the metal, all three detectors registered the maximum of elution peaks at  $t_r$  34 min (Fig. 1f). Evidently, the amount of gold nanoparticles could be held by isolated molecules of the polysaccharide, and did not form large aggregates. Molecular mass and polydispersity index of AG were constant within limits of the method accuracy upon the composite formation (see table). When the metal content was increased to 11.9%, the retention time of the eluted gold nanoparticles (plasmon resonance registered with spectrophotometer detector) was of  $t_r$  32 min (Fig. 1g). RI could register the free AG molecules at  $t_r$  35 min; simultaneously,  $M_p$  ( $t_r$  37.5) and  $M_n$  (35.1 kDa) decreased, the polydispersity index being up to 1.38. Besides that peak, light scattering detector revealed appearance of two additional peaks at higher  $M$  range with the retention times of 26.0 and 29.5 min. The fraction of aggregated molecules in that nanocomposite increased to reach 35%. In another study, light scattering of the Au-AG composite (10% Au) marked the presence of large aggregates and dimeric nanoparticles [13]; that was evidently detected in this work in SEC experiment.

Definitely, the nature of metal influences the composite formation process, but the attempts to quantify the effect accounting for the metal redox potential (by comparison of the molecular parameters of silver- and gold-containing composites with the same content of metal) failed. Reduction of  $\text{HAuCl}_4$  and  $\text{AgNO}_3$  into the zero-valence metals required different amount of the reducing agent but that did not influence the AG degradation as marked by the close values of  $M_p$  (see table); the sharp change of  $M_n$  [18.50 (Ag) and 35.09 kDa (Au)] leading to the enhanced polydispersity was not correlated with the redox potential  $E^0$  of the precursors (0.564 V, Ag and 1.000 V, gold). Likely, that could be explained by the mechanism of reduction of the multi-stage reduction of  $\text{HAuCl}_4$  into Au via a series of intermediates  $[\text{Au}(\text{OH})\text{Cl}_3]^-$ ,  $[\text{Au}(\text{OH})_2\text{Cl}_2]^-$ ,  $[\text{Au}(\text{OH})_3\text{Cl}]^-$ , and  $[\text{Au}(\text{OH})_4]^-$ , each stage showing its own redox potential [21].

The changes in molecular mass distribution were more prominent in the cases of high-molecular

polysaccharides with low branching degree, GM and CG. In particular, the Ag-GM nanocomposite with 7.0% of silver (Fig. 2b) revealed molecular mass of 45.6 kDa ( $t_r$  34.6 min) with significant fraction of degraded macromolecules ( $M_n$  38.0) and, consequently, increased polydispersity degree of 2.35. Light scattering detector showed three peaks with retention time of 27.0, 29.6, and 34.0 min, thus pointing at the presence of aggregated macromolecules. The calculated radius of the aggregates was decreased from 27 to 14 nm upon the composite formation, due to a combination of redox reaction and alkali-induced depolymerization.

In the case of Au-GM composite containing 4.2% of gold (Fig. 2c), the  $M_w$  value was of 193.7 kDa, reflecting the fraction of long-chain molecules in the presence of deeply degraded macromolecules ( $M_n$  65.6 kDa). Consequently, the polydispersity increase up to 2.95 was more prominent than that in the case of similar silver-containing composite. The macromolecules mass in the elution peak ( $t_r$  33.2 min) was two-fold decreased ( $M_p$  62.5 kDa) as compared with the parent GM ( $M_p$  120.5 kDa). Light scattering detector registered two peaks with  $t_r$  of 26.0 and 32.0 min, confirming the presence of aggregated macromolecules. The calculated aggregate radius was up to 34 nm. The composites of GM clearly marked the effect of increasing metal content (4.2 and 7.0%) on the molecular mass decrease in the course of the composite formation. The presence of oligomer fractions ( $t_r$  44.0 min) in the GM composites was again due to the alkali-induced depolymerization enhanced by the redox processes.

The changes of polysaccharide molecular mass were even more prominent upon formation of the composites with CG. For example, the Ag-CG composite containing 4.0% of the metal (table and Fig. 3b), revealed the molecular mass of  $M_p$  55.9 kDa ( $t_r$  34.2 min). The polysaccharide was relatively monodisperse (1.22) and contained the macromolecules significantly degraded upon the composite formation. Light scattering detector registered two peaks with  $t_r$  of 26.4 and 34.2 min, pointing at the presence of 1–2% of macromolecules aggregated with silver nanoparticles.

In the case of the Au-CG composite containing 6.0% of gold (Fig. 3c), the polysaccharide showed molecular mass of  $M_p$  102.5 kDa ( $t_r$  30 min), becoming highly degraded and more narrow disperse (1.35) as

well (see table). Light scattering detector registered the only peak with  $t_r$  28.4 min. No peak of the aggregated macromolecules was observed; the calculated radius of CG macromolecules in the Au-CG composite was of 33 nm.

To conclude, GM and CG, being initially more high-molecular as compared with AG, were degraded much deeper in the course of the composites formation. As the preparation conditions were always the same, the reason for that was definitely a different structure of the polysaccharides. The glycoside linkage type is known to affect the rate of alkali-induced depolymerization. In particular, the  $\beta$ -(1 $\rightarrow$ 4)-glycoside linkages are more sensitive towards hydrolysis [22]. A special feature of CG was sharp decrease of the polydispersity degree upon formation of the nanocomposites (AG and GM became more polydisperse upon the composite preparation). Likely, CG was easier degraded in the alkaline medium due to a different type of the glycoside linkage and the regular linear structure, in contrast to the highly branched AG and GM.

The SEC analysis taking advantage of hyphenated three-detector technique was extremely informative mean to study the changes of molar mass parameters in the course of formation of metal nanocomposites with polysaccharides. In particular, it was shown that the composites formation was accompanied by the decrease of molecular mass of the polymers and change of their polydispersity index, due to a combination of redox reactions involving the noble metals precursors and the alkali-induced degradation. The interaction of metal nanoparticles with the macromolecules of the stabilizer was directly confirmed. The nature and the content of the metal both influenced the observed changes of the polymer molecular parameters. In detail, increase of the metal nanoparticles amount enhanced the fraction of aggregated macromolecules in the sample. The degradation processes were majorly reflected in the molecular mass decrease in the cases of GM and CG. Self-assembly of the nanoparticles and the macromolecule to form a nanocomposite is a result of a set of factors including the dimensional effect of the nanoparticles.

## EXPERIMENTAL

Galactomannan GM (LBG brand) was isolated from *Ceratonia siliqua*; carrageenan CG (WR-78 CP

Celko Aps brand, Denmark) was isolated from *Rhodomela lycopodioides*; arabinogalactan AG was isolated from *Larix sibirica* via water extraction and precipitation in ethanol as described elsewhere [14].

The silver- (Ag-AG, Ag-GM, and Ag-CG) and gold-containing (Au-AG, Au-GM, and Au-CG) composites based on polysaccharides matrices were prepared as described earlier [9, 10]. The metal content in the composites (3.7–11.9 wt %) was determined via atom absorption method using an Analyst 200 Perkin-Elmer spectrometer.

Molar mass parameters of the parent polysaccharides and the nanocomposites were determined by means of high-pressure size-exclusion chromatography using an Agilent 1100/1260 liquid chromatograph with two tandem columns Ultrahydrogel Linear (Waters, USA), 300 mm long with inner diameter of 8 mm. The solutions were filtered through nylon filter Sartorius (Germany) with pores of 0.45  $\mu$ m before injection. Concentration of the analyzed samples was of 1–4 mg/mL, the injected volume being of 100  $\mu$ L. 0.1 mol/L aqueous solution of sodium nitrate was used as eluent, the flow rate being of 0.5 mL/min. The columns and detectors temperature was maintained at 40°C. Detection was performed in the three-channel mode using a differential refractometer (RID10A, Shimadzu), a multi-angle light scattering detector (Mini DAWN TriStar, Wyatt Technology Corporation, USA), and a spectrophotometer at 200–600 nm. The low-disperse polyethylene oxides and PSS pullulans (Germany) were used as standards for calibration [18]. SEC results were processed taking advantage of the Astra 5.3.4.20 software.

## ACKNOWLEDGMENTS

This work was financially supported by Russian Foundation for Basic Research (project no. 14-43-04127 r\_sibir\_a).

## REFERENCES

1. Pomogailo, A.D. and Kestelman, V.N., *Metallopolymer Nano-Composites*, Berlin, Heidelberg; New York: Springer, 2005.
2. Krutyakov, Yu.A., Kudrinskiy, A.A., Olenin, A.Yu., and Lisichkin, G.V., *Russ. Chem. Rev.*, 2008, vol. 77, no. 3, p. 233. DOI: 10.1070/RC2008v077n03ABEH003751.
3. Khlebtsov, N. and Dykman, L., *Chem. Soc. Rev.*, 2011, vol. 40, p. 1647. DOI: 10.1039/C0CS00018C.
4. Daniel, M.-C. and Astruc, D., *Chem. Rev.*, 2004, vol. 104, no. 1, p. 293. DOI: 10.1021/cr030698+.



5. Giljohann, D., Seferos, D., Daniel, W., Massich, M., Patel, P., and Mirkin, C., *Angew. Chem. Int. Ed.*, 2010, vol. 49, no. 19, p. 3280. DOI: 10.1002/anie.200904359.
6. Dreaden, E., Alkilany, A., Huang, X., Murphy, C., and El-Sayed, M., *Chem. Soc. Rev.*, 2012, vol. 41, p. 2740. DOI: 10.1039/c1cs15237h.
7. Kumar, A., Zhang, X., and Liang, X.-J., *Biotech. Adv.*, 2013, vol. 31, p. 593. DOI: 10.1016/j.biotechadv.2012.10.002.
8. RF Patent 2260500, 2005, *Byull. Izobret*, 2005, c. 26.
9. Sukhov, B.G., Aleksandrova, G.P., Grishchenko, L.A., Feoktistova, L.P., Sapozhnikov, A.N., Proidakova, O.A., T'kov, A.V., Medvedeva, S.A., and Trofimov, B.A., *Russ. J. Struct. Chem.*, 2007, vol. 48, no. 5, p. 922. DOI: 10.1007/s10947-007-0136-3.
10. Lesnichaya, M.V., Aleksandrova, G.P., Feoktistova, L.P., Sapozhnikov, A.N., Fadeeva, T.V., Sukhov, B.G., and Trofimov, B.A., *Russ. Chem. Bull.*, 2010, vol. 59, no. 12, p. 2323.
11. Lesnichaya, M.V., Aleksandrova, G.P., Feoktistova, L.P., Sapozhnikov, A.N., Sukhov, B.G., and Trofimov, B.A., *Dokl. Chem.*, 2011, vol. 440, p. 282. DOI: 0.1134/S0012500811100065.
12. Grishchenko, L.A., Medvedeva, S.A., Aleksandrova, G.P., Feoktistova, L.P., Sapozhnikov, A.N., Sukhov, B.G., and Trofimov, B.A., *Russ. J. Gen. Chem.*, 2006, vol. 76, no. 7, p. 1111. DOI: 10.1134/S1070363206070189.
13. Gasilova, E., Khripunov, A., Toropova, A., Bushin, S., Grishchenko, L., and Aleksandrova, G., *J. Phys. Chem. (B)*, 2010, vol. 114, no. 12, p. 4204. DOI: 10.1021/jp100018q.
14. Dubrovina, V.I., Medvedeva, S.A., Vityazeva, S.A., Kolesnikova, O.B., Aleksandrova, G.P., Gutsol, L.O., Grishchenko, L.A., and Chetveryakova, T.D., *Struktura i immunomoduliruyushchee deistvie arabinogalaktana listvennitsy sibirskoi i ego metalloproduktov* (Structure and Immunomodulatory Effects of Siberian Larch Arabinogalactan and Its Metal Derivatives), Irkutsk: Asprint, 2007.
15. Shcherbukhin, V.D. and Anulov, O.V., *Prikl. Biokhim. i Mikrobiol.*, 1999, vol. 35, no. 3, p. 257.
16. Yarockii, S.V., Shashkov, A.S., and Usov, A.I., *Bioorg. Khim.*, 1978, no. 4, p. 745.
17. Azarov, V.I., Burov, A.V., and Obolenskaya, A.V., *Khimiya drevesiny i sinteticheskikh polimerov* (Wood Chemistry and Synthetic Polymers), St. Petersburg: S.-Peterburg. Lesotekhnich. Akad., 1999.
18. Boymirzaev, A.S., Shomurotov, Sh., and Turaev, A., *Khim. Rast. Syr'ya*, 2013, no. 2, p. 51.
19. Boymirzaev, A.S., *Khim. Rast. Syr'ya*, 2009, no. 2, p. 19.
20. Aleksandrova, G.P., Grishchenko, L.A., Fadeeva, T.V., Sukhov, B.G., and Trofimov B.A., *Nanotekhnika*, 2010, vol. 23, no. 3, p. 34.
21. Xiaohui Ji, Xiangning Song, Jun Li, Yubai Bai, Wensheng Yang, Xiaogang Peng, *J. Am. Chem. Soc.*, 2007, 129, p. 13939. DOI: 10.1021/ja074447k.
22. Fengel, D. and Wegener, G., *Wood Chemistry, Ultrastructure, Reactions*, Berlin: Walter de Gruyter, 1984.